UNIVERSIDADE TECNOLÓGICA FEDERAL DO PARANÁ

MAURICELLE SONYA KANA NGUEMO

ESTABILIDADE EM TEMPO FINITO DE SISTEMAS LINEARES COM PARÂMETROS VARIANTES NO TEMPO: ABORDAGEM ALEATÓRIA.

CORNÉLIO PROCÓPIO

2024

MAURICELLE SONYA KANA NGUEMO

ESTABILIDADE EM TEMPO FINITO DE SISTEMAS LINEARES COM PARÂMETROS VARIANTES NO TEMPO: ABORDAGEM ALEATÓRIA.

Finite-time stability of linear systems with time-varying parameters: randomized approach.

Dissertação apresentado como requisito para obtenção do título de Mestrado em Engenharia Elétrica do Programa de Pós-Graduação em Engenharia Elétrica da Universidade Tecnológica Federal do Paraná.

Orientador: Prof. Dr. Alessandro do Nascimento Vargas

Coorientador: Prof. Dr. Cristiano Marcos Agulhari

CORNÉLIO PROCÓPIO

2024

4.0 Internacional

Esta licença permite download e compartilhamento do trabalho desde que sejam atribuídos créditos ao(s) autor(es), sem a possibilidade de alterá-lo ou utilizá-lo para fins comerciais. Conteúdos elaborados por terceiros, citados e referenciados nesta obra não são cobertos pela licença.

Ministério da Educação
Universidade Tecnológica Federal do Paraná
Campus Cornélio Procópio

MAURICELLE SONYA KANA NGUEMO

ESTABILIDADE EM TEMPO FINITO DE SISTEMAS LINEARES COM PARÂMETROS VARIANTES NO TEMPO: ABORDAGEM ALEATÓRIA

Trabalho de pesquisa de mestrado apresentado como requisito para obtenção do título de Mestre Em Engenharia Elétrica da Universidade Tecnológica Federal do Paraná (UTFPR). Área de concentração: Sistemas Eletrônicos Industriais.

Data de aprovação: 29 de Julho de 2024

Dr. Alessandro Do Nascimento Vargas, Doutorado - Universidade Tecnológica Federal do Paraná

Dr. Cristiano Marcos Agulhari, Doutorado - Universidade Tecnológica Federal do Paraná

Dr. Marcio Aurelio Furtado Montezuma, Doutorado - Universidade Tecnológica Federal do Paraná

Dr. Ricardo Coracao De Leao Fontoura De Oliveira, Doutorado - Universidade Estadual de Campinas (Unicamp)

Documento gerado pelo Sistema Acadêmico da UTFPR a partir dos dados da Ata de Defesa em 01/08/2024.

Dedico este trabalho aos meus pais e irmãos,
pelo amor, carinho e incentivo.

AGRADECIMENTOS

Agradeço, primeiramente, a Deus, por me dar o dom da vida, saúde, paz e sabedoria, iluminando meu caminho, guiando-me e zelando-me, e à Virgem Maria, por me proteger e abençoar-me todos os dias.

Aos meus pais, Maurice Kana e Solange Metiokeng Nguefack, por me darem amor, carinho, incentivo, apoio imensurável, e oportunidade de estudo, não medindo esforços para me proporcionarem uma vida melhor.

Gostaria de expressar minha profunda gratidão aos meus irmãos e irmãs por estarem sempre ao meu lado. Sua presença, apoio e amor incondicional têm sido fundamentais em cada etapa da minha jornada. Agradeço por compartilharmos momentos de alegria, superação e crescimento juntos.

Agradeço aos amigos que o mestrado me proporcionou e, com os quais, dividi bons momentos de alegria, felicidade, conversas, e principalmente aprendizado e companheirismo. Agradeço também pelos demais amigos que a UTFPR me proporcionou, e que se tornaram para mim, nada menos que uma família.

Agradeço também ao Professor Dr. Alessandro do Nascimento Vargas pela grande orientação, ensinamentos e conselhos, os quais contribuíram grandemente para minha formação pessoal e profissional. Agradeço também ao Professor Dr. Cristiano Marcos Agulhari, pela colaboração e contribuição para o desenvolvimento deste trabalho, bem como os ensinamentos proporcionados.

Quero expressar minha sincera gratidão aos membros da banca por aceitarem dedicar seu tempo e expertise para avaliar meu trabalho. Sua disposição em fornecer *feedback* e orientação é inestimável para o meu desenvolvimento acadêmico e profissional. Agradeço profundamente pela oportunidade de compartilhar minhas ideias e contribuições com vocês.

Agradeço a todos meus mestres e professores, os quais contribuíram para minha formação, bem como a Universidade Tecnológica Federal do Paraná (UTFPR), câmpus Cornélio Procópio, e a Coordenação de Aperfeiçoamento de Pessoal de Nível Superior (CAPES), por toda estrutura e ajuda de custo disponibilizada para o desenvolvimento deste trabalho.

Por fim, agradeço a todos que, neste período, tive a oportunidade de conhecer e conviver, a cada um que me fez pensar e aprender mais um pouco sobre a vida e sobre este pequeno mundo.

La vie n'est facile pour aucun de nous. Mais quoi, il faut avoir de la persévérance, et surtout de la confiance en soi. Il faut croire que l'on est doué pour quelque chose, et que, cette chose, il faut l'atteindre coûte que coûte (CURIE, 1937).

RESUMO

O objetivo deste trabalho é desenvolver uma nova abordagem para verificar a estabilidade em tempo finito de sistemas lineares com parâmetros variantes no tempo (*Linear Parameter-Varying (LPV)*). Aplicando o método clássico de Lyapunov, são derivadas condições suficientes para garantir a estabilidade em tempo finito para classes maiores de sistemas variantes no tempo, estendendo-se além do escopo dos resultados existentes. O conceito de estabilidade contrativa em T-passos, adaptado aos sistemas LPV, é desenvolvido. Como o problema de contração otimizada demanda um esforço computacional proibitivo mesmo para valores pequenos de T, é aplicada uma abordagem aleatória para sua resolução. A estabilidade contrativa robusta em T-passos de sistemas LPV em um tempo finito é testada em termos de um problema de factibilidade envolvendo desigualdades matriciais lineares (*Linear Matrix Inequalities (LMIs)*). A abordagem aleatória é capaz de assegurar a factibilidade do problema de otimização com uma alta margem de probabilidade, fornecendo um algoritmo de teste que garante a estabilidade contrativa do sistema em T-passos dentro de um tempo finito. O uso do algoritmo de Mayne, um caso específico do filtro de Kalman, para a identificação do amortecedor magneto-reológico (*Magnetoreological (MR)*) tem se mostrado muito benéfico, resultanto na identificação do sistema com um erro de menos de 0,001%. Um controlador foi desenvolvido e adaptado a um sistema de amortecedor MR acoplado a uma mesa vibrante para validar experimentalmente as teorias de estabilidade discutidas neste trabalho, resultando em dados obtidos por experimentos em tempo real.

Palavras-chave: sistemas lineares com parâmetros variantes no tempo; estabilidade robusta; amortecedor magneto-reológico; estabilidade em tempo finito; desigualdades matriciais lineares.

ABSTRACT

The aim of this work is to develop a new strategy to check the finite-time stability of linear parameter-varying (LPV) systems. By applying the classical Lyapunov method, sufficient conditions are derived to ensure finite-time stability for larger classes of time-varying systems, extending beyond the scope of existing results. The concept of contractive stability in T-steps adapted to LPV systems has been developed. As the optimized contraction problem demands a prohibitive computational burden even for small values of T, a randomized approach is applied to solve it. The robust finite-time contractive stability of LPV systems in T-steps is tested in terms of a feasibility problem involving linear matrix inequalities (LMIs). The randomized approach is able to ensure the feasibility of the optimization problem with a high degree of probability, providing a test algorithm that guarantees the contractive stability of the system in T-steps within a finite time. The use of the Mayne's algorithm, a specific case of Kalman filter, for the identification of MR damper has proved very beneficial, resulting in the system identification with an error of less than 0.001%. A controller was designed and adapted to an MR damper system coupled to a shaking table to experimentally validate the stability theories discussed in this work, resulting in data obtained from real-time experiments.

Keywords: linear parameter-varying systems; robust stability; magnetorheological damper; finite-time stability; linear matrix inequalities.

LISTA DE ABREVIATURAS E SIGLAS

Siglas

CAPES	Coordenação de Aperfeiçoamento de Pessoal de Nível Superior
FTS	Finite-Time Stability
LMIs	Linear Matrix Inequalities
LPV	Linear Parameter-Varying
LTI	Linear Time Invariant
LTV	Linear Time-Varying
MR	Magnetoreological
PWM	Pulse Width Modulation
RMSE	Root Mean Square Error
UTFPR	Universidade Tecnológica Federal do Paraná

CONTENTS

1 INTRODUÇÃO

Os sistemas lineares com parâmetros variantes no tempo (LPV) apresentam um comportamento dinâmico que muda linearmente com determinados parâmetros, permitindo uma representação mais precisa de sistemas complexos em comparação com os modelos tradicionais lineares invariantes no tempo (*Linear Time Invariant (LTI)*) (ZHANG; WANG; WANG, 2023; ZHU; ZHENG, 2023). A utilidade dos sistemas LPV se estende por uma infinidade de aplicações de engenharia, refletindo sua adaptabilidade para capturar as variações dinâmicas inerentes aos sistemas do mundo real (ZHANG; WANG; WANG, 2023). Em áreas como engenharia aeroespacial, sistemas automotivos, robótica e controle de processos, os modelos LPV têm sido ferramentas indispensáveis para enfrentar os desafios associados a variações de parâmetros, incertezas e não linearidades (DANIELSON; KLOEPPEL; PETERSEN, 2023).

Com relação à estabilidade dos sistemas LPV, os pesquisadores têm explorado diferentes abordagens (ZHANG; HAN; GE, 2021; AGULHARI *et al.*, 2013). É interessante notar que uma abordagem comum para verificar a estabilidade dos sistemas LPV é baseada em desigualdades matriciais lineares (*LMIs*); veja os livros (DUAN; YU, 2013; EFIMOV; RAISSI; ZOLGHADRI, 2013; GHAOUI; NICULESCU, 1999) e os artigos (GEROMEL, 2023; LI; FU, 1997; PANDEY; OLIVEIRA, 2018; ROSA; MORAIS; OLIVEIRA, 2018; WU, 2001) para obter mais detalhes. As LMIs oferecem uma abordagem sistemática e computacionalmente tratável para resolver problemas de controle complexos, permitindo a formulação de condições de estabilidade, síntese de controladores e especificações de desempenho (BERTOLIN *et al.*, 2018; SOUZA *et al.*, 2022). A adoção de LMIs facilitou avanços significativos no projeto e na análise de sistemas de controle LPV, oferecendo uma estrutura matemática rigorosa para abordar requisitos de estabilidade, robustez e desempenho (GHAOUI; NICULESCU, 1999; ROTONDO; NEJJARI; PUIG, 2014; VANANTWERP; BRAATZ, 2000).

A estabilidade em tempo finito (*Finite-Time Stability (FTS)*), um aspecto essencial da análise de sistemas, também chama a atenção no contexto dos sistemas LPV (AMATO *et al.*, 2014; LI; YANG; SONG, 2019). A FTS surgiu como um conceito de estabilidade para sistemas não lineares (WEISS; INFANTE, 1967), e logo se tornou popular também para sistemas lineares (AMATO *et al.*, 2010; MA; WU; WANG, 2016).

Vários estudos recentes começaram a investigar a estabilidade em tempo finito para sistemas LPV, contribuindo para o cenário em evolução das metodologias de análise de estabilidade. Por exemplo, (AMATO *et al.*, 2014) investigaram a FTS para sistemas lineares discretos e variantes no tempo (DT-LTV). Seu trabalho estabeleceu um conjunto de condições, baseadas na resolução de desigualdades matriciais lineares a diferença (DLMI) que, se satisfeitas, garantem a FTS do sistema.

O trabalho (ZHOU, 2020) explora a aplicação da estabilização em tempo finito de sistemas lineares usando uma estrutura de realimentação linear com variação de tempo limitada. Por meio da teoria de estabilidade de Lyapunov, esse artigo demonstra que uma função de alto

ganho variante no tempo pode levar a tempos de convergência significativamente mais rápidos. A eficiência dessa abordagem é validada por meio de simulações numéricas.

Em 2021, (CHAIB-DRAA *et al.*, 2021) propuseram novas técnicas de estimativa de tempo finito para sistemas LPV de tempo discreto. Eles se concentram na estabilidade com realimentação de saída e apresentam dois métodos de estimativa: o uso dos estados do sistema com atraso com base em um algoritmo de estimativa explícito e o uso de dois observadores assintóticos combinados, ligados por uma condição de inversibilidade de uma determinada matriz variante no tempo, para recuperar a solução do sistema LPV em tempo finito. As simulações verificaram a validade e a eficiência dos resultados obtidos.

(GUNASEKARAN *et al.*, 2023) apresentaram em 2023 a teoria de FTS para um modelo epidêmico compartimental estocástico, definindo compartimentos suscetíveis-infectados-recuperados e sinais de mudança. Eles usaram um sistema LPV para examinar o comportamento da infecção a longo prazo. Usando a teoria da estabilidade de Lyapunov, os autores estabeleceram a resposta mais adequada para o controle eficaz da pandemia da COVID-19. Há muitos outros trabalhos sobre o tópico da FTS (por exemplo, (BAI *et al.*, 2024; LIU; YANG; LI, 2015; NIE *et al.*, 2022; XU; ZHANG; QI, 2023)).

Além das técnicas tradicionais de análise de estabilidade, as abordagens aleatórias surgiram como ferramentas promissoras para lidar com a dinâmica e as incertezas de sistemas complexos (CALAFIORE; FAGIANO, 2013; VARGAS *et al.*, 2019). A aplicação de algoritmos randomizados a sistemas LPV oferece oportunidades para soluções de controle robustas e dimensionáveis. Pesquisas recentes exploraram o potencial de abordagens aleatórias no contexto de modelagem e controle, destacando sua eficácia na atenuação dos efeitos de variação de parâmetros e distúrbios (VARGAS *et al.*, 2019; YU; BIANCHI; PIRODDI, 2023).

1.1 Justificativa

Apesar do progresso feito na compreensão das propriedades de estabilidade e das estratégias de controle dos sistemas LPV, algumas áreas de pesquisa permanecem relativamente inexploradas. Especialmente, a questão da FTS contrativa em T-passos para sistemas dinâmicos LPV tem recebido pouca atenção na literatura. Note que a estabilidade contrativa em horizonte infinito garante a convergência das trajetórias para um ponto de equilíbrio, e representa um aspecto essencial de sistemas dinâmicos (Veja, (SASTRY, 2013, chap. 1) e (KHALIL, 2002, Sec. 2.1)). No entanto, nenhuma metodologia foi proposta para abordar a estabilidade contrativa em T-passos para sistemas dinâmicos LPV, ressaltando a necessidade de mais pesquisas nessa área.

1.2 Objetivo

O principal objetivo deste trabalho é caracterizar a estabilidade em tempo finito especificamente aplicável aos sistemas dinâmicos LPV, ou seja, a estabilidade contrativa em T-passos. Por meio de uma abordagem aleatória, assegura-se que o sistema se contraia e dissipe energia, em T-passos, com uma margem de probabilidade alta.

Não se consegue resolver o problema de estabilidade robusta LPV com 100% de certeza. Porém, a abordagem proposta consegue garantir uma probabilidade alta, por exemplo, superior a 99,9%. Em outras palavras, podemos garantir que o sistema contrai em T-passos com 99,9% de chance.

Este trabalho contém uma aplicação para um amortecedor magneto-rheológico (MR). Este amortecedor foi acoplado a uma mesa vibrante, e dados experimentais foram colhidos (kit composto de amortecedor MR acoplado a mesa vibrante).

O estimador de Mayne, um caso particular do filtro de Kalman, é usado para obter um sistema linear variante no tempo. Usando os dados do experimento realizado, verificamos que o método de identificação de Mayne apresentou um erro de identificação inferior a 0,001%.

Por fim, um controle robusto do tipo proporcional e integrador (P+I), utilizando a abordagem aleatória é desenvolvido e aplicado ao dispositivo do amortecedor MR acoplado à mesa vibrante, cujo objetivo é controlar a posição da mesa.

1.2.1 Objetivos Específicos

- (Experimental) Obter a base de dados por experimentos em malha aberta efetuados em tempo real numa mesa vibrante conectada a um amortecedor MR;
- (Algoritmo) Aplicar o estimador de Mayne nos dados experimentais para a identificação do sistema LPV;
- (Algoritmo) Desenvolver um método de *clustering* para reduzir a quantidade de matrizes (parâmetros) obtidas no método de Mayne;
- (Teoria) Estabelecer as condições de estabilidade contrativa em tempo finito de um sistema LPV;
- (Algoritmo) Implementar o método de abordagem randomizada;
- (Numérico) Achar os parâmetros de resolução das LMIs com o controle desenvolvido;
- (Experimental) Implementar o controle no kit de laboratório.

1.3 Organização do trabalho

Este documento é dividido em sete capítulos, que são:

- Capítulo 1 — Apresenta a introdução, e expõe a revisão da literatura sobre os sistemas LPV e o conceito de estabilidade em tempo finito;
- Capítulo 2 — Expõe a abordagem de estabilidade robusta em tempo finito dos sistemas lineares e variantes no tempo (*Linear Time-Varying (LTV)*). Este capítulo traz a contribuição de uma abordagem de estabilidade contrativa em T-passos de sistemas LTV;
- Capítulo 3 — Desenvolve um algoritmo aleatório para a resolução do problema de otimização baseado na estabilidade contrativa do sistema e apresenta a análise da factibilidade e síntese das LMIs;
- Capítulo 4 — Expõe a identificação dos sistemas lineares e variantes no tempo usando o método de Mayne; Um algoritmo de *clustering* também é apresentado;
- Capítulo 5 — Apresenta os experimentos *real-time* em malha aberta: amortecedor MR acoplado a uma mesa vibratória; Neste capítulo é apresentado o equipamento do laboratório e sua identificação;
- Capítulo 6 — Apresenta os experimentos *real-time* em malha fechada. Neste capítulo é implementado o controle no kit de laboratório;
- Capítulo 7 — Traz as conclusões finais, bem como as respectivas perspectivas para futuros aprimoramentos do trabalho.

1.4 Notações

O símbolo $\mathbb{R}$ denota o conjunto de números reais. O espaço linear normalizado de todas as matrizes reais $n \times m$ é denotado por $\mathbb{R}^{n,m}$. A notação $\|\cdot\|$ denota a norma euclidiana padrão em $\mathbb{R}^n$ ou a norma de Frobenius em $\mathbb{R}^{n,m}$. A cardinalidade de um conjunto S é denotada por $card(S)$. O símbolo $(')$ denota a operação de transposição. O raio espectral de uma matriz $U \in \mathbb{R}^{n,n}$ é denotado por $\sigma(U)$ (maior valor absoluto dos seus autovalores).

2 PRELIMINARIES AND PROBLEM FORMULATION

2.1 Linear parameter-varying systems

Consider the following autonomous LPV system:

$$x_{k+1} = A(\alpha_k)x_k, \quad x_0 \in \mathbb{R}^n, \quad \forall k \geq 0, \tag{1}$$

where $x_k \in \mathbb{R}^n$ denotes the system state, and the matrix $A(\alpha_k)$ depends affinely on the time-varying parameter α_k, which takes values from the unit simplex

$$\Lambda = \left\{ \alpha \in \mathbb{R}^\eta : \sum_{i=1}^{\eta} \alpha_i = 1,\ \alpha_i \geq 0,\ i = 1,\ldots,\eta \right\}, \tag{2}$$

where $\eta > 0$ represents the number of vertices. The affine condition on $A(\cdot)$ means that

$$A(\alpha_k) = \sum_{i=1}^{\eta} \alpha_{k,i} A_i, \quad \alpha_k \in \Lambda, \tag{3}$$

where $A_0, \ldots, A_\eta$ are given matrices.

The goal of this chapter is to show conditions that characterize the finite-time stability of the LPV system (1).

2.2 Robust finite-time stability

The next stability concept comes from a straightforward adaptation of the classical definition of finite-time stability (e.g., (AMATO; ARIOLA; COSENTINO, 2010, Defn. 1), (AMATO; ARIOLA, 2005, Defn. 1), (AMATO; ARIOLA; DORATO, 2001, Defn. 1)).

Definition 2.2.1. *(Robust finite-time stability) Given positive scalars c_1 and c_2, with $c_1 < c_2$, we say* (1) *is robustly finite-time stable with respect to (c_1,c_2,T) provided that*

$$\|x_0\| \leq c_1 \Rightarrow \|x_k\| < c_2, \quad k = 1,2,\ldots,T. \tag{4}$$

Since (1) is a linear system that has a finite expansion in each step, we can find constants c_1 and c_2 that satisfy (4) whenever $T > 0$ is finite. As a result, (1) satisfies the condition in 2.2.1. To see this, apply the norm on both sides of (1) to obtain

$$\|x_k\| = \|A(\alpha_{k-1})x_{k-1}\| \leq \sup_{\alpha \in \Lambda} \|A(\alpha)\| \|x_{k-1}\|.$$

Iterating the last expression yields

$$\|x_k\| \leq \left(\sup_{\alpha\in\Lambda} \|A(\alpha)\|\right)^k \|x_0\|, \quad \forall k > 0,$$

which results that $\|x_k\|$ is bounded from above by a finite constant whenever $\|x_0\|$ and k are finite numbers. This argument shows that robust FTS does not prevent a system from expanding and eventually diverging, thus reaching an unstable behavior in the long run; see (AMATO; ARIOLA, 2005, Rem. 1). For this reason, we decided to associate the LPV system with a stronger stability concept: *contractiveness in finite time*.

This stability concept means the system contracts after a finite number of steps; namely, the system diminishes its initial energy—at least once—when passing through the T-th step, as defined next.

Definition 2.2.2. *The system* (1) *is contractive stable in T-steps if there exists a constant* $0 < \xi < 1$ *such that*

$$\|x_T\|^2 < \xi\|x_0\|^2. \tag{5}$$

The following theorem states alternative conditions that characterizes the contractive stability of system (1)

Theorem 2.2.1. *Given three positive constants* c_0*,* c_1*, and* c_2*, suppose that there exist a function* $P : \Lambda \mapsto \mathbb{R}^{n\times n}$ *and a constant* $T > 0$ *such that* $\forall \alpha_0, \alpha_1, \ldots, \alpha_T \in \Lambda$

$$c_2 I_n - P(\alpha_T) < 0, \quad P(\alpha_0) - c_1 I_n < 0, \quad Z(\alpha_{k+1},\alpha_k) < 0, \quad k = 0,\ldots,T-1, \tag{6}$$

where

$$Z(\alpha_{k+1}, \alpha_k) := A(\alpha_k)'P(\alpha_{k+1})A(\alpha_k) - (1 - c_0)P(\alpha_k). \tag{7}$$

Then the system (1) *is contractive stable in T-steps provided that*

$$\frac{c_1}{c_2}(1 - c_0)^T < 1.$$

Proof Define the Lyapunov function $V(x_k)$ as (e.g.,(DAAFOUZ; BERNUSSOU, 2001, Thm. 1))

$$V(x_k) = x_k'P(\alpha_k)x_k, \quad k = 1,\ldots,T. \tag{8}$$

Multiplying left- and right-hand sides of $Z(\alpha_{k+1},\alpha_k)$ by x_k' and x_k, respectively, we obtain

$$x_k'A(\alpha_k)'P(\alpha_{k+1})A(\alpha_k)x_k - (1 - c_0)x_k'P(\alpha_k)x_k < 0, \tag{9}$$

which results in

$$V(x_{k+1}) < (1 - c_0)V(x_k).$$

Iterating this inequality on $k = 0, \ldots, T-1$ yields

$$V(x_T) < (1 - c_0)^T V(x_0). \tag{10}$$

Because (6) mensures that $\lambda_{\max}(P(\alpha_0)) < c_1$ and $\lambda_{\min}(P(\alpha_T)) > c_2$, we can use (10) to write

$$|x_T|^2 < \frac{c_1}{c_2}(1 - c_0)^T |x_0|^2. \tag{11}$$

The contractive stability result then follows by setting $\xi = c_1(1 - c_0)^T / c_2$ in (11) with $\xi < 1$ (see Definition 2.2.2).

Remark 2.2.1. *The problem mentioned in equation* (6) *is numerically intractable. To overcome this difficulty, we resort to a randomized approach, detailled in the following Chapter.*

3 RANDOMIZED APPROACH

3.1 Definition and algorithm

The randomized approach, also known as *s*cenario approach (e.g., (CALAFIORE; CAMPI, 2005; TEMPO; CALAFIORE; DABBENE, 2013)), represents a method that converts hard-to-solve deterministic problems into a sampling-based problem (e.g., (TEMPO; CALAFIORE; DABBENE, 2013, Sec. 13.1.1, p. 193)). The randomized approach determines that random samples, extracted from the polytopic set, are fed directly into an optimization problem (e.g., (CALAFIORE; CAMPI, 2005; CAMPI; GARATTI, 2011; CAMPI; GARATTI, 2008; SCHILDBACH; FAGIANO; MORARI, 2013; TEMPO; CALAFIORE; DABBENE, 2013)). The optimization problem then considers these random samples (i.e., scenarios) instead of the whole uncertain set, allowing the computation of the solution from a finite number of elements.

In the setup of this work, the randomized approach applies as follows. We randomly draw the elements $\alpha_0, \ldots, \alpha_T$ from Λ, and check whether (6) is feasible. If the answer is positive, we repeat this random experiment and check again whether (6) is feasible. While repeating this experiment many times, we keep observing if the outcome for the random sample remains feasible. In the end, if the outcome remains feasible for all trials, we can say that *it is likely* that the result of Theorem 2.2.1 holds true for all values of $\alpha_T, \ldots, \alpha_T$ belonging to Λ. However, the word "*likely*" is imprecise and needs further clarification, which is done in the next section.

3.2 Contractive stability as an optimization problem

In this section, we convert the inequalities (6) into an optimization problem. For this purpose, we need some additional notation and definition. Let us define the T-times cartesian product of Λ, say,

$$\Omega_T = \underbrace{\Lambda \times \cdots \times \Lambda}_{T\text{-times}}.$$

Suppose that the conditions of Theorem 2.2.1 are valid with $P : \Lambda \mapsto \mathbb{R}^{n\times n}$ as a linear function of α. In this case, there exist symmetric, positive definite matrices $P_1, \ldots, P_\eta \in \mathbb{R}^{n\times n}$ such that the affine parameter-dependent matrix

$$P(\alpha_k) = \sum_{i=1}^{\eta} \alpha_{k,i} P_i, \quad \alpha_k \in \Lambda, \tag{12}$$

satisfies the inequalities (6) for all $\alpha = (\alpha_0, \ldots, \alpha_T) \in \Omega_T$. Because of that, we can choose a sufficiently small constant $\rho < 0$ such that

$$(c_2 - \rho)I_n - P(\alpha_T) \leq 0, \quad P(\alpha_0) - (c_1 + \rho)I_n \leq 0, \quad Z(\alpha_{k+1},\alpha_k) - \rho I_n \leq 0, \\ k = 0, \ldots, T-1. \quad (13)$$

Define the spectral raduis $\sigma(\cdot)$ as the largest absolute value of the eigenvalues of one matrix. The inequalities in (13) allow us to borrow an idea from (VARGAS *et al.*, 2019, Sec. 2), and recast (13) as an optimization problem. Namely, define the functional $f : (-\infty,0) \times \Omega_T \mapsto \mathbb{R}^n$ as

$$f(\rho,\alpha) \; = \; \max\{f_1(\rho,\alpha), f_2(\rho,\alpha), f_3(\rho,\alpha)\}, \quad \forall \alpha \in \Omega_T, \; \forall \rho < 0, \quad (14)$$

where

$$f_1(\rho,\alpha) = \sigma\left((c_2 - \rho)I_n - P(\alpha_T)\right), \\ f_2(\rho,\alpha) = \sigma\left(P(\alpha_0) - (c_1 + \rho)I_n\right), \\ f_3(\rho,\alpha) = \max_{k=0,\ldots,T-1} \left\{\sigma\left(Z(\alpha_{k+1},\alpha_k) - \rho I_n\right)\right\}.$$

Then, consider the following optimization problem.

$$\text{Minimize } \rho < 0 \text{ subject to } f(\rho,\alpha) \leq 0, \; \forall \alpha \in \Omega_T. \quad (15)$$

The next result is an immediate consequence of Theorem 2.2.1.

Corollary 3.2.1. *If the optimization problem* (15) *is feasible, then* (1) *is contractive stable in* T *steps.*

Remark 3.2.1. *Although Corollary 3.2.1 shows an elegant way to check the contractive stability of the LPV system* (1)*, such approach remains useless from a computational viewpoint because it depends on infinitely many values of* $\alpha \in \Omega_T$*. To circumvent this difficulty, we convert* (15) *into a simpler-to-handle problem, i.e., the random sampling-based problem.*

3.3 The sampling-based problem

The next set of assumptions and definitions are quite standard in the theory of the randomized approach; see further details, for instance, in (CALAFIORE; CAMPI, 2005; CAMPI; GARATTI, 2011; CAMPI; GARATTI, 2008; SCHILDBACH; FAGIANO; MORARI, 2013; TEMPO; CALAFIORE; DABBENE, 2013; VARGAS *et al.*, 2019).

Assumption 3.3.1. *((VARGAS et al., 2019, Assump. 1)). The set Ω_T is endowed with some σ-algebra, and $\mathbb{P}$ denotes the corresponding probability measure.*

Definition 3.3.1. *(Probability of violation, e.g., (CAMPI; GARATTI, 2011, Defn. 2.2), (VARGAS et al., 2019, Defn. 2.2)). Given some $\rho < 0$, the probability of violation is defined as*

$$H(\rho) = \mathbb{P}\{\alpha \in \Omega_T : f(\rho,\alpha) > 0\}.$$

Definition 3.3.2. *(β-level solution, e.g., (CAMPI; GARATTI, 2008, p. 1212),(VARGAS et al., 2019)). Given any $\beta \in (0,1)$, we say that $\rho < 0$ is a β-level solution if $H(\rho) \leq \beta$.*

As quoted by the authors of (VARGAS *et al.*, 2019), Definitions 3.3.1 and 3.3.2 together imply that we must accept the risk of finding some "bad" elements $\tilde{\rho} < 0$ and $\tilde{\alpha} \in \Omega$ such that $f(\tilde{\rho},\tilde{\alpha}) > 0$, which violates (15). This is a well-known drawback when using the randomized approach (CALAFIORE; CAMPI, 2005; CAMPI; GARATTI, 2011; CAMPI; GARATTI, 2008; SCHILDBACH; FAGIANO; MORARI, 2013; TEMPO; CALAFIORE; DABBENE, 2013). However, a way to decrease the chance of observing such "bad" elements is to set $\beta > 0$ extremely small, as quoted in (VARGAS *et al.*, 2019, Rem. 4), yet smaller values of β imply in more samples to be processed (e.g., (CALAFIORE; CAMPI, 2005; CAMPI; GARATTI, 2011; CAMPI; GARATTI, 2008; SCHILDBACH; FAGIANO; MORARI, 2013; TEMPO; CALAFIORE; DABBENE, 2013)), thus resulting in a tradeoff between the accuracy of the solutions and numerical complexity.

The next definition is a straightforward adaptation of (VARGAS *et al.*, 2019, Defn. 2.4).

Definition 3.3.3. *(Randomized algorithm). Assume that the elements $\alpha^{(\ell)} \in \Omega_T$, $\ell = 0,\ldots,S$, are taken independent and identically distributed according to a given probability measure $\mathbb{P}$. Solve the convex optimization problem:*

$$\textit{Minimize } \rho < 0 \textit{ subject to } f(\rho,\alpha^{(\ell)}) \leq 0,\ \ell = 0,\ldots,S. \tag{16}$$

Proposition 3.3.1. *(VARGAS et al., 2019, Prop. 2.5) Consider a feasible solution of the random convex problem in* (16) *and denote it by ρ_S^*. Then*

$$\mathbb{P}^S\{H(\rho_S^*) > \beta\} \leq (1-\beta)^S, \tag{17}$$

where $\mathbb{P}^S = \mathbb{P} \times \cdots \times \mathbb{P}$, and S denotes the number of sampling elements.

Remark 3.3.1. *The number of sampling elements S plays a crucial role in randomized algorithms (CALAFIORE; CAMPI, 2005, Thm. 1): the larger the number S, the greater the probability of observing $H(\rho_S^*) < \beta$, which ensures that $\rho_S^* > 0$ is an β-level solution (VARGAS et al., 2019, Rem. 5). A drawback, though, is that increasing S also increases the computational complexity of solving the convex problem* (16) *(e.g., (TEMPO; CALAFIORE; DABBENE, 2004, Chap.*

13.1.1)). Getting samples and solving this problem becomes a overdemanding process when S is too large. The randomized approach then presents a trade-off between complexity and computational burden, a challenge to users who wish $\beta > 0$ excessively small.

In Chapter 6, we illustrate the usefulness of the randomized approach through a real-time application.

4 IDENTIFICATION OF TIME-VARYING LINEAR SYSTEMS

This chapter presents a method to identify the stochastic LTV system

$$x_{k+1} = A_k x_k + B_k u_k + v_k, \quad k \geq 0, \quad x_0 \in \mathbb{R}^n, \tag{18}$$

where $x_k \in \mathbb{R}^n$ represents the system state, $u_k \in \mathbb{R}^m$ denotes the input, and $\{v_k\}$ on $\mathbb{R}^n$ denotes a zero-mean Gaussian process with known covariance matrix $R_k = \mathrm{E}[v_k v_k']$ for all $k \geq 0$. We assume that (i) the pair of matrices (A_k,B_k) on $(\mathbb{R}^{n\times n}, \mathbb{R}^{n\times m})$ is unknown, and (ii) the values of both x_k and u_k are measured perfectly without measurement errors. Under these assumptions, the identification problem consists of finding matrices (A_k,B_k) that best fit the dynamics (18).

To compute (A_k,B_k), we employ Mayne's method (MAYNE, 1963), which essentially is a particular case of the Kalman filter (DANIEL, 1976, Sec. 12.4, pg. 208). As suggested by the method (FREEMAN; HASSAN; MORTON., 1986; MAYNE, 1963), define the system output as

$$y_k = x_{k+1}, \quad \forall k \geq 0. \tag{19}$$

As a result,

$$y_k = A_k x_k + B_k u_k + v_k, \quad \forall k \geq 0. \tag{20}$$

The terms of the above equation can be recast as (e.g., (FREEMAN; HASSAN; MORTON., 1986; MAYNE, 1963))

$$y_k = \varphi_k' \theta_k + v_k. \tag{21}$$

To illustrate how to represent (18) as (21), consider the system (18) with dimension two, i.e.,

$$A_k = \begin{bmatrix} a_{11,k} & a_{12,k} \\ a_{21,k} & a_{22,k} \end{bmatrix}, \quad B_k = \begin{bmatrix} b_{1,k} \\ b_{2,k} \end{bmatrix}.$$

For this particular case, we can write

$$\varphi_k' = \begin{bmatrix} x_{1,k} & x_{2,k} & 0 & 0 & u_{1,k} & 0 \\ 0 & 0 & x_{1,k} & x_{2,k} & 0 & u_{1,k} \end{bmatrix}, \quad \theta_k = \begin{bmatrix} a_{11,k} & a_{12,k} & a_{21,k} & a_{22,k} & b_{1,k} & b_{2,k} \end{bmatrix}'.$$

Note that (18) and (21) are equivalent. In the notation (21), φ_k contains the measurement data and θ_k consists of the parameters to be estimated.

Now, we can apply Mayne's method to identify θ_k, $k \geq 0$, according to the literature (FREEMAN; HASSAN; MORTON., 1986; MAYNE, 1963). Consider

$$\theta_k = \theta_{k-1} + w_{k-1}, \quad \forall k > 0, \tag{22}$$

where $\{w_k\}$ stands for a Gaussian process with covariance matrices satisfying $Q_k = \mathrm{E}[w_k w_k']$ and $\mathrm{E}[w_k v_k'] = 0$, for all $k \geq 0$.

Remark 4.0.1. *Mayne's estimator was initially designed with $w_k \equiv 0$ and $Q_k \equiv 0$, since it was designed to deal with time-invariant matrices, i.e., $A_k \equiv A$ and $B_k \equiv 0$; see (MAYNE, 1963). Considering $\{w_k\}$ in* (22) *allows us to adapt Mayne's estimator to the identification of the time-varying linear system* (18)*.*

Let $\hat{\theta}_k$ be the optimal estimator for the system in (22). It follows that $\hat{\theta}_k$ can be computed through the observed information y_k from (21), i.e.,

$$\hat{\theta}_k = \hat{\theta}_{k-1} + G_k e_k, \tag{23}$$

where $e_k = y_k - \varphi_k' \hat{\theta}_{k-1}$, and

$$\begin{aligned} G_k &= L_{k-1}\varphi_k(\varphi_k' L_{k-1}\varphi_k + R_k)^{-1}, \\ L_k &= L_{k-1} - G_k \varphi_k' L_{k-1} + Q_k. \end{aligned} \tag{24}$$

Note that the recurrence (22)–(24) constitute Mayne's estimator (FREEMAN; HASSAN; MORTON., 1986; MAYNE, 1963), which coincides with the Kalman filter equations (DANIEL, 1976, Sec. 12.4, pg. 208).

4.1 Clustering matrices

The identification algorithm (22)–(24) allows us to obtain the pair (A_k,B_k), $k = 0,\ldots,N$, whenever the corresponding data (x_k,u_k), $k = 0,\ldots,N$, is available. However, when N is sufficiently large, we start facing a computational problem: how to effectively process the large number of matrices (A_k,B_k). To help alleviate this computational problem, we apply the clustering method to the matrices (A_k,B_k), as detailed next.

The clustering method chooses certain matrices to become the *cluster points*. All the remaining matrices, which are close enough to a cluster point, will be discarded. For example, set $\varepsilon > 0$ as *the clustering radius*, and consider $M_k = [A_k \; B_k]$, $k = 0,\ldots,9$, as depicted in Figure 1. Note that M_0 centers a ball of radius of ε that encompasses M_2 and M_6; consequently, M_0 is a cluster point. Similarly, M_1 and M_7 are cluster points, representing balls that

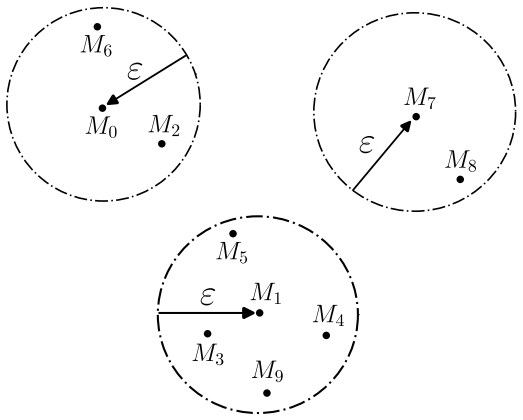

Figure 1 – Illustration of cluster points.

encompasse (M_3,M_4,M_5,M_9) and M_8, respectively. In summary, M_0, M_1, and M_7 are cluster points representing all points $M_0, \ldots, M_9$ within a range distance of at least ε.

Next, we formalize the clustering algorithm.

- *Step 1*: Given $\varepsilon > 0$ and $M_k = [A_k\ B_k]$, $k = 0, \ldots N$, choose any index k_0 and set the corresponding matrix M_{k_0} to be the first cluster point, that is, $\tilde{\mathcal{M}} = \{M_{k_0}\}$. The algorithm generates the cluster set $\tilde{\mathcal{M}} = \{\tilde{M}_0, \ldots, \tilde{M}_m\}$ with $m < N$, as follows. Set $k = 0$ and go to the next step.

- *Step 2*: Enumerate the cluster set as $\tilde{\mathcal{M}} = \{\tilde{M}_0, \ldots, \tilde{M}_m\}$, and compute

$$d = \min_{i=0,\ldots,m} \left\| M_k - \tilde{M}_i \right\|$$

  where $m = card(\tilde{\mathcal{M}}) - 1$. If $d > \varepsilon$, then set $\tilde{\mathcal{M}} = \tilde{\mathcal{M}} \cup \{M_k\}$. Set $k = k + 1$ and go to the next step.

- *Step 3*: If $k = N + 1$, then stop the algorithm; otherwise, return to *Step 2*.

Remark 4.1.1. *The clustering algorithm ensures two properties: (i) given any matrix M_k, we can choose a cluster point $M_{i_0} \in \tilde{\mathcal{M}}$ such that $\|M_k - M_{i_0}\| < \varepsilon$; and (ii) all cluster points are far from each other by a distance of at least ε.*

4.2 Error analysis: the cluster-based representation for the system parameters

According to the clustering algorithm, for each $M_k = [A_k\ B_k]$, $k = 0, \ldots, N$, there exist corresponding cluster points $\tilde{M}_{i_0}, \ldots, \tilde{M}_{i_N}$ on $\tilde{\mathcal{M}}$ such that (see Remark 4.1.1)

$$\|M_k - M_{i_k}\| < \varepsilon, \quad k = 0, \ldots, N. \tag{25}$$

Defining $[\tilde{A}_k\ \tilde{B}_k] = \tilde{M}_{i_k}$, $k = 0, \ldots, N$, we can recast the system (18) as

$$x_{k+1} = \tilde{A}_k x_k + \tilde{B}_k u_k + e_k + v_k, \tag{26}$$

where $e_k := (A_k - \tilde{A}_k)x_k + (B_k - \tilde{B}_k)u_k$. The term e_k accounts for the error the clustering method induces.

Remark 4.2.1. *The experimental data, to be presented in Section 5.3, suggest that* $\{e_k\}$ *tends to follow a Gaussian distribution.*

Remark 4.2.2. *Note that the identification method of Chapter 4 generates the pairs* (A_k,B_k) *for* $k = 0, \ldots, N$*. When applying this identification method in practice, we almost always obtain time-varying matrices with values different from each other, that is,* $(A_i,B_i) \neq (A_j,B_j)$ *for all* $i \neq j$*. However, the clustering method ensures that* $(\tilde{A}_i, \tilde{B}_i) = (\tilde{A}_j, \tilde{B}_j)$*, for some elements* i *and* j*, because the cardinality of the set* $\tilde{\mathcal{M}}$ *tends to be much less than* N*. As the experimental application of Chapter 5 illustrates, the cluster points* $\tilde{\mathcal{M}}$ *become the vertices of the polytope representing the LPV system.*

5 MAGNETORHEOLOGICAL DAMPER ATTACHED TO A SHAKING TABLE: OPEN-LOOP IDENTIFICATION

MR dampers are innovative damping devices that dynamically adjust their stiffness in response to an external magnetic field, providing an adaptable and responsive solution for attenuating vibrations and shocks in a variety of applications (DANIEL *et al.*, 2018; MASA'ID *et al.*, 2023; YUAN *et al.*, 2019). MR dampers stand out as intelligent devices, offering considerable potential for the semi-active control of structures (HA; ROYEL; BALAGUER, 2018; KHALID *et al.*, 2014). When attached to shaking tables, in particular, they can emulate relevant processes, such as earthquakes or vibrations in vehicles (MASA'ID *et al.*, 2023; ŞAHIN *et al.*, 2021; VARGAS *et al.*, 2022). In this section, we present data extracted from an MR damper attached to a shaking table. This equipment, from now on, is called simply as "*MR shaking table*."

This section aims to identify a model for the MR shaking table. Given the highly nonlinear characteristics of MR dampers (CHEN; NIE; YU, 2022; DOMINGUEZ; SEDAGHATI; STIHARU, 2008; PENG; YANG; LI, 2018; ZHANG *et al.*, 2023), the task of modeling such dynamics poses significant challenges. For example, even the modern hysteresis-based Bouc-Wen models exhibit up to 20% of identification error (CHAE; RICLES; SAUSE, 2013; DOMINGUEZ; SEDAGHATI; STIHARU, 2006; LI; WANG, 2011; VARGAS *et al.*, 2022). Given the complexity of modeling MR dampers, characterized by their nonlinear behavior, we foresee the LPV framework as an interesting tool for representing MR dampers, motivated by the fact that an LPV system can encompasse complex dynamics using relatively simple representation. Representing nonlinear systems in the LPV framework is supported by studies such as (ABBAS *et al.*, 2021; ARMANINI; KARÁSEK; VISSER, 2018; CASAVOLA; FAMULARO; FRANZÈ, 2003; EFIMOV; RAISSI; ZOLGHADRI, 2013), which highlight the advantages of LPV modeling, its accuracy, and enhanced computational efficiency. Next, we show experimental data that support this idea.

5.1 Laboratory setup

Experiments were carried out in a laboratory setup containing an MR damper attached to a shaking table (VARGAS *et al.*, 2022). The MR damper was physically connected to the left side of the table; the right side was connected to a linear actuator; see Figures 2 and 3.

The pieces and parts used in the experiments are as follows. The table was made with a steel plate base measuring 980mm long, 300mm wide, and 25.4mm thick; an MR fluid damper model RD-8041-1, manufactured by Lord Corporation (Cary, NC, USA); a data acquisition card manufactured by National Instruments (NI) (Austin, TX, USA), model NI PCI-6221; an actuator in the form of a Glideforce model LACTT12P-12V-20 Light-Duty, linear ball screw actuator (Las Vegas, NV, USA). The actuator has a maximum displacement of 457mm, a maximum current load of 13.2A; a sliding platform is 303mm long, 300mm wide and 15.87mm thick; two linear rails to support the sliding platform; a KA-300 linear encoder, manufactured by Sino (Suzhou,

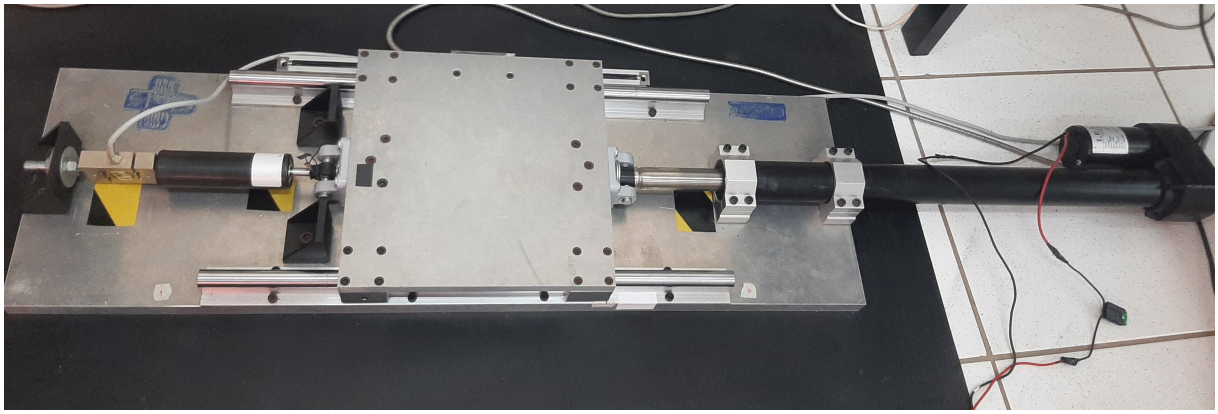

Figure 2 – Shaking table apparatus. Attached to the table are a magnetorheological damper (left) and a linear actuator (right).

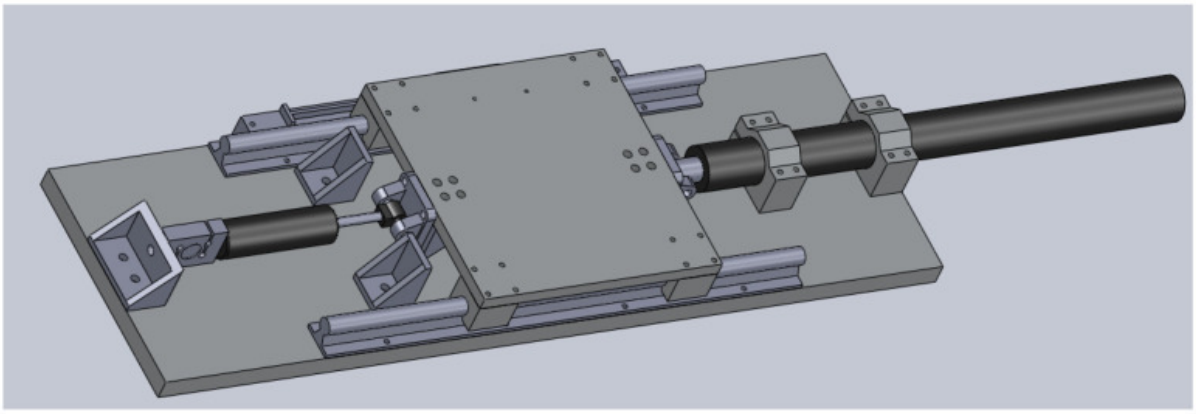

Figure 3 – Pictural representation of the shaking table apparatus (VARGAS *et al.*, 2022).

Jiangsu, China), with a scale precision of 5 μm and a measuring range of 370mm. A high-power H-Bridge model IBT-4 (50A) Pulse Width Modulation (PWM) motor drive received a PWM signal from the NI acquisition board. A car's battery of 12V supplied the circuit. The shaking table operates as a single-axis device, comprising a base and a sliding table. An actuator controls the sliding table's movement along its central axis, while an MR damper and load cell measure forces exerted during motion. The top platform of the shaking table, linked to the actuator, experiences controlled left-to-right and right-to-left motions. A linear encoder tracks platform displacement, providing precise position measurements.

5.2 Identification of the MR shaking table

Let us consider the system (20), i.e.,

$$x_{k+1} = A_k x_k + B_k u_k + v_k, \quad k \geq 0, \quad x_0 \in \mathbb{R}^n, \tag{27}$$

where x_k denotes the states vector, u_k is the control input, and v_k is a Gaussian error.

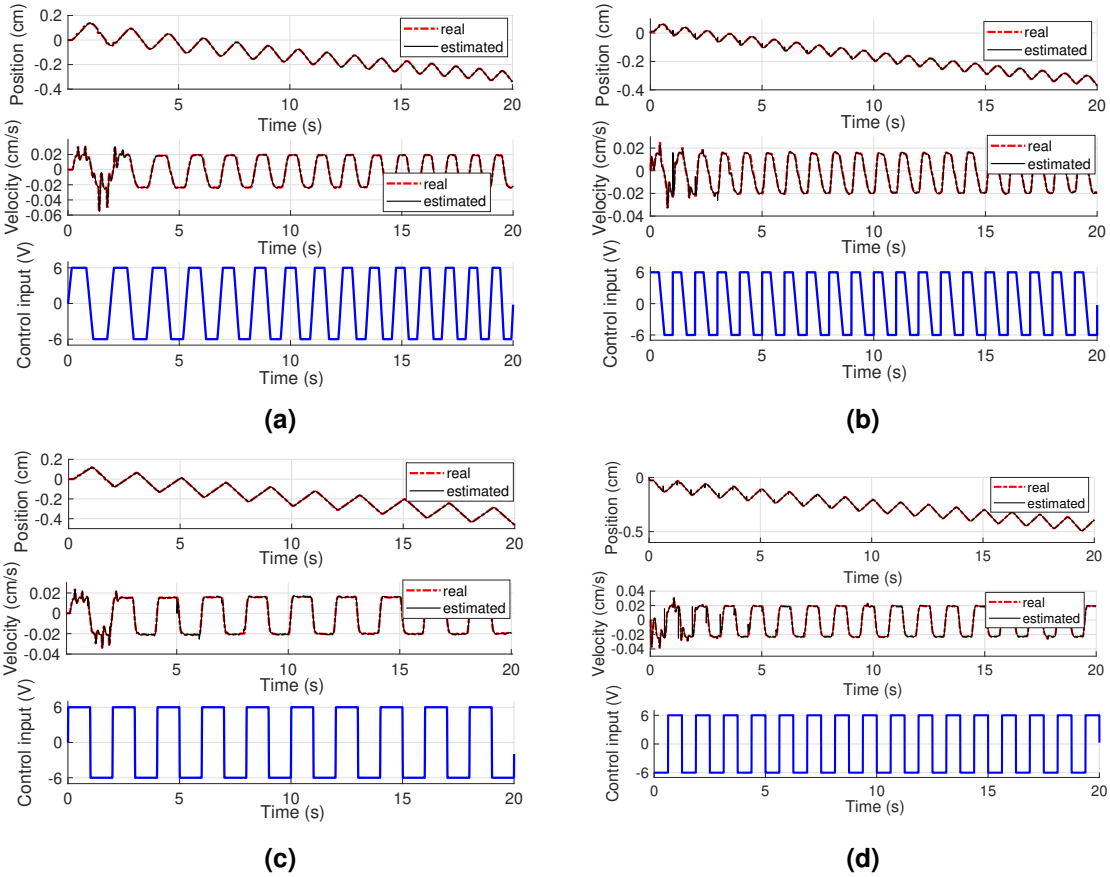

Figure 4 – Data for MR shaking table. Pictures show real-time data and their estimated counterpart for position x_1 (cm) and velocity x_2 (cm per second).

A series of experiments were performed on the MR shaking table to find matrices A_k, B_k that best represent its dynamical behavior (see Chapter 4). The experimental procedure is described as follows. Fifty different open-loop experiments were performed using different sources of excitation, including sine, chirp, square, sawtooth, and random signals, with different amplitudes (cm) and frequencies (Hz).

Data for position (cm) and velocity (cm per second) were recorded and stored, representing $x_{1,k}$ and $x_{2,k}$, respectively. This data was used in the identification algorithm described by equations (22)–(24).

Figure 4 shows four samples for the position $x_{1,k}$, the velocity $x_{2,k}$ and the co

ntrol input u_k of the MR shaking table. As can be seen, the curves show the system response for (a) a chirp excitation with an initial frequency of 0.5Hz and a final frequency of 1Hz; (b) a sawtooth with a fixed frequency of 1Hz; (c) sine wave with a fixed frequency of 0.5Hz; and (d) square wave with a fixed frequency of 0.8Hz. Here, the input u_k controls the system with a saturation of 6V. In red is the real-time data, and in black is the estimated data performed using Mayne's filter described in Chapter 4. This process is validated by computing the Root Mean Square Error (RMSE) between the actual data and the estimated data. This RMSE in the identification is negligible, i.e., less than 0.001%.

As can be seen in Figure 4, the position tended to decrease as time evolved. This can be attributed to the properties of the magnetorheological fluid inside the damper. Namely, the force applied in one direction produces a displacement; the same force applied in the opposite direction produces a completely different displacement, an effect caused by hysteresis (SNYDER; KAMATH; WERELEY, 2001; WEI; WANG; OU, 2021; TSOUROUKDISSIAN *et al.*, 2009).

5.3 Experimental error introduced by clustering

Since fifty different open-loop experiments were performed, and each experiment contains 4,000 points, we end up with about 200,000 pairs of matrices (A_k,B_k). To reduce this large number of matrices, as checking the system stability, we employ the algorithm in *Steps 1–3* with $\varepsilon = 0.1$ (Section 4.1).

It resulted in a cluster set $\tilde{\mathcal{M}} = \{\tilde{M}_0, \ldots, \tilde{M}_m\}$ with $m = 655$ (see Remark 6.3.2). This means that we reduced the number of matrices under analysis from 200,000 to 655.

Accordingly, the cluster set corresponds to the pair of matrices $(\tilde{A}_k,\tilde{B}_k)$ such that the system (27) equals (see Section 4.2)

$$x_{k+1} = \tilde{A}_k x_k + \tilde{B}_k u_k + e_k + v_k, \quad \forall k \geq 0, \tag{28}$$

where the error

$$e_k = (A_k - \tilde{A}_k)x_k + (B_k - \tilde{B}_k)u_k, \quad \forall k \geq 0, \tag{29}$$

was computed and stored (Remark 6.3.2), see a summary in Figure 5. As can be observed in the histogram of Figure 5, the error e_k seems to approximate a Gaussian distribution. If we assume that position and velocity are Gaussian variables, then they have mean $\mu_1 = -0.072$ and $\mu_2 = 10^{-04}$ and standard deviation $\Sigma_1 = 0.047$ and $\Sigma_2 = 6.3 \times 10^{-4}$, respectively. The next chapter dives deeper into this assumption.

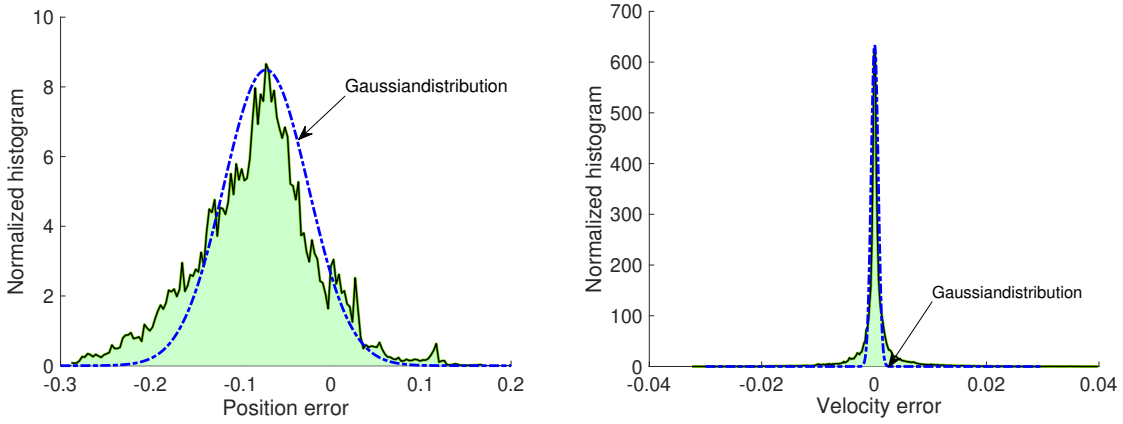

(a) **(b)**

Figure 5 – Error introduced by the clustering method (see (29)**): histogram (green) and Gaussian curve fit (blue).**

6 REAL-TIME CLOSED-LOOP EXPERIMENTS

This chapter illustrates the importance of the randomized approach in a real-time application. The randomized approach was applied in a closed-loop control experiment involving a magnetorheological damper attached to a shaking table (MR shaking table). The controller is designed to assure the contractive stability of the closed loop dynamics. Experimental data support the usefulness of the randomized approach defined in Chapter 3, as described next.

6.1 Linear parameter-varying system representing the MR shaking table

Let $(\tilde{A}_i,\tilde{B}_i)$, $i = 0,\ldots,m$, be the cluster points obtained in Section 5.3. We can use these cluster points to define the affine matrices

$$A(\alpha_k) = \sum_{i=1}^{\eta} \alpha_{k,i}\tilde{A}_i, \quad B(\alpha_k) = \sum_{i=1}^{\eta} \alpha_{k,i}\tilde{B}_i, \quad \forall \alpha_k \in \Lambda. \tag{30}$$

The next assumption is key to the experiments performed in the MR shaking table.

Assumption 6.1.1. *The linear parameter-varying system*

$$x_{k+1} = A(\alpha_k)x_k + B(\alpha_k)u_k + w_k, \quad x_0 \in \mathbb{R}^n, \quad \forall k \geq 0, \tag{31}$$

represents the dynamics of the MR shaking table, where $\{w_k\}$ is an i.i.d. Gaussian process with mean and covariance satisfying the relation $w_k = e_k + v_k$ (see Section 5.3).

Remark 6.1.1. *MR dampers are nonlinear and complex devices—they have dynamics that are hard to identify. In Chapter 5, we used a deterministic time-varying linear system that was able to characterize certain features of the MR shaking table. As explained in Chapter 5, this system generated an error w_k, $k \geq 0$, that resembles a Gaussian variable. This motivated us to consider $\{w_k\}$ as an i.i.d. Gaussian process.*

6.2 Closed-loop strategy

To implement the closed-loop strategy for the LPV system (31), we deploy the linear state-feedback control associated with an integrator, as depicted in Figure 6 (see (OSTERTAG, 2011, Sec. 1.8.2.3). The control input is given by:

$$u_k = [K_1\ K_2]x_k + K_3 q_k, \quad \forall k \geq 0, \tag{32}$$

where $K = [K_1\ K_2\ K_3] \in \mathbb{R}^3$ represents a control gain to be chosen later.

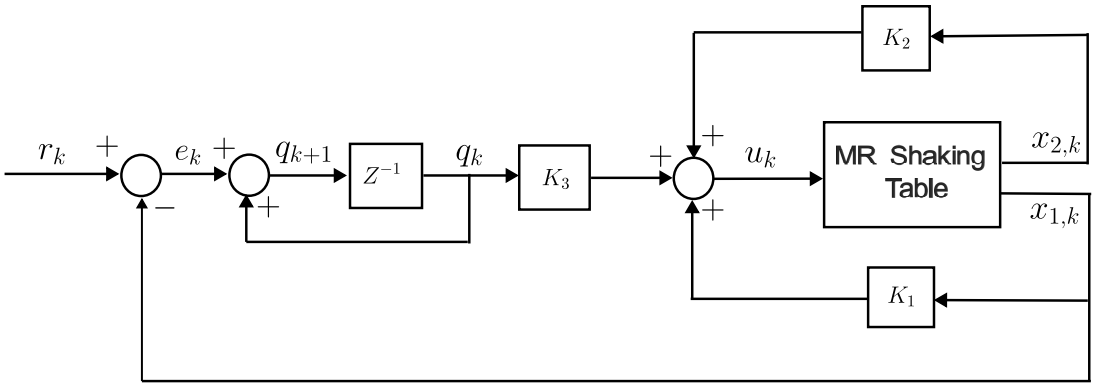

Figure 6 – Control of the MR shaking table.

As can be seen in Fig. 6, the following difference equation defines the discrete integrator $q_k \in \mathbb{R}$:

$$q_{k+1} = q_k + r_k - x_{1,k}, \quad k \geq 0, \tag{33}$$

where r_k (cm) represents the reference input signal for the position of the MR shaking table. Substituting (32) and (33) into (31) gives

$$\begin{bmatrix} x_{k+1} \\ q_{k+1} \end{bmatrix} = \hat{A}(\alpha_k, K) \begin{bmatrix} x_k \\ q_k \end{bmatrix} + \begin{bmatrix} w_k \\ r_k \end{bmatrix}, \quad \alpha_k \in \Lambda, \quad \forall k \geq 0, \quad x_0 \in \mathbb{R}^n, \tag{34}$$

where the closed-loop system matrix is defined as

$$\hat{A}(\alpha_k, K) = \begin{bmatrix} A(\alpha_k) + B(\alpha_k)[K_1 \; K_2] & B(\alpha_k)K_3 \\ [-1 \; 0] & 1 \end{bmatrix}. \tag{35}$$

6.2.1 Stability analysis

Note that the system state $\{x_k\}$ from (34) is a stochastic process because it depends on the Gaussian process $\{w_k\}$. Studying stochastic stability is out of the scope of this work—this topic will be considered in future work. This work focuses only on the deterministic version of (34); namely, we consider (34) with $r_k \equiv 0$ and $w_k \equiv 0$, which equals

$$x_{k+1} = \hat{A}(\alpha_k, K)x_k, \quad \alpha_k \in \Lambda, \quad \forall k \geq 0, \quad x_0 \in \mathbb{R}^n. \tag{36}$$

The goal here is to ensure that (36) is contractive stable in T-steps (Definition 2.2.2). Because this task is computationally impossible to solve (Remark 2.2.1), we employ the randomized approach (Chapter 3).

Even with the help of the randomized approach, we have to acknowledge that the stability of (36) depends on which gain K is chosen in the closed-loop matrix $\hat{A}(\alpha_k, K)$. We advance this discussion in the next section.

6.3 Results and discussion

This section illustrates the usefulness of the randomized approach for checking that (36) is contractive stable in T-steps with a certain probability margin. The procedure for the randomized experiment is describe as follows.

We used a trial-and-error process to choose certain parameters that were important to the randomization test: we used trial-and-error to find the control gain $K = [0.5\ 0.1\ 60]$ and the constants $c_0 = 10^{-4}$, $c_1 = 0.998$, $c_2 = 0.999$, and $T = 8$ (see Theorem 2.2.1). We considered the randomized algorithm of Definition 3.3.3 with S equal to 250,000 samples, and the corresponding optimization problem in (16) was feasible (with ρ_S^* less than 10^{-3}), within a time simulation of 109 hours 19 minutes and 12 seconds. This feasibility of (16) has the following implications.

Suppose we accept the risk of finding some "bad" elements $\tilde{\alpha} \in \Omega$ that could potentially deny the property of contractive stability. Suppose, in addition, that this risk is minimal, say, $\beta = 9 \times 10^{-5}$. It follows from Proposition 3.3.1 that

$$\mathbb{P}^S\{H(\rho_S^*) > \beta\} \leq (1-\beta)^S = 1.690 \times 10^{-10}. \tag{37}$$

This negligible number in (37) ensures that our previous assumption about "bad" elements is correct. Namely, these numbers mean that the probability that (36) is contractive stable in T-steps is at least 99.995%.

Remark 6.3.1. *The numerical experiments were performed using a computer with the following configurations: an Intel Core i7 14700 Central Processing Unit (CPU), 16GB of RAM, and Ubuntu 24.04 64-bits operating system. The software setup includes MATLAB® version 2023a, the LMI solver MOSEK ApS (2019) version 10.0.26, and the LMI parser YALMIP (LOFBERG, 2004).*

6.3.1 Experimental data

Figure 7 shows the experimental representation of the closed-loop control implemented on the MR shaking table kit using the gain K. We can observe that the curve representing the table's position (black) follows the reference signal r_k (red). Furthermore, as the Definition 2.2.2 on contractive stability indicates, we can see that the system tends to zero when $r_k \equiv 0$, thus confirming the contraction property.

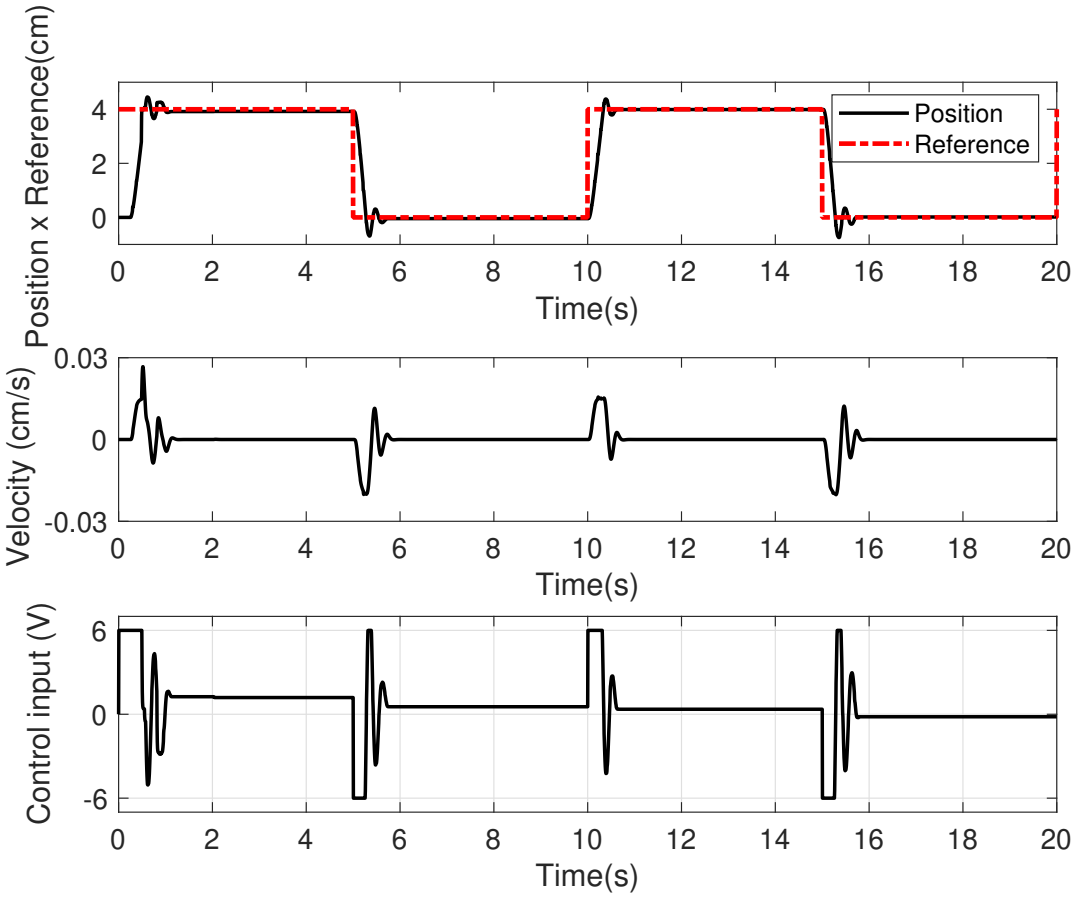

Figure 7 – Real-time closed-loop experiment.

Remark 6.3.2. *All the Data, source codes, and files used in this manuscript are freely available on GitHub to download at www.github.com/ labcontrol-data/ randomized_LPV_shakingTable.*

7 CONCLUSÃO GERAL E PERSPECTIVAS

Este trabalho caracterizou a estabilidade em tempo finito (FTS) de sistemas lineares com parâmetros variantes no tempo (LPV). O principal conceito de estabilidade é chamado de estabilidade contrativa de T-passos, que exige que o sistema seja contrativo em um tempo finito $T > 0$.

Sabe-se que verificar a estabilidade dos sistemas LPV é um problema difícil, pois requer a solução de um problema de otimização com complexidade computacional proibitiva para os computadores atuais. No entanto, foi demonstrado que uma abordagem aleatória pode superar esta dificuldade. A abordagem aleatória requer a factibilidade do problema de otimização, dentro de uma margem de probabilidade. Se o problema de otimização for factível para um número elevado de amostras, então pode-se garantir a estabilidade contrativa em T-passos do sistema com garantia de certa margem de probabilidade.

Do ponto de vista experimental, um amortecedor MR foi acoplado a uma mesa vibrante para ilustrar a abordagem aleatória. Esse kit experimental gerou dados que foram usandos no estimador de Mayne. O objetivo foi obter um sistema linear variante no tempo, para posteriormente converter esse sistema em um sistema LPV. A aplicação de um controle de tipo proporcional e integrador (P+I) no sistema permitiu de avaliar experimentalmente a estabilidade robusta contrativa em tempo finito com certa margem de probabilidade.

7.1 Perspectivas

Como perspectivas de trabalho futuro, planeja-se:

- Escrever um artigo para publicação numa revista científica, contribuindo assim para o avanço da pesquisa na área de estabilidade de sistemas LPV sob abordagem aleatória;
- Estudar como técnicas LMIs podem ser incorporadas no controle robusto de sistemas LPV sob abordagem aleatória;
- Estudar se o raio espectral $\sigma(A(\alpha_T) \dots A(\alpha_0)) < 1$ é um tópico de interesse na abordagem aleatória, pois os autovalores de uma matriz são calculados mais rapidamente do que resolver LMIs.

BIBLIOGRAPHY

ABBAS, H. S. *et al.* LPV modeling of nonlinear systems: A multi-path feedback linearization approach. **International Journal of Robust and Nonlinear Control**, Wiley Online Library, v. 31, n. 18, p. 9436–9465, 2021.

AGULHARI, C. M. *et al.* $\mathcal{H}\infty$ dynamic output feedback for LPV systems subject to inexactly measured scheduling parameters. *In*: IEEE. **2013 American control conference**. Washington, DC, USA, 2013. p. 6060–6065.

AMATO, F. *et al.* **FTS of Discrete-Time Linear Systems**. London: Springer London, 2014. 53-66 p. ISBN 978-1-4471-5664-2.

AMATO, F. *et al.* Input–output finite time stabilization of linear systems. **Automatica**, Elsevier, v. 46, n. 9, p. 1558–1562, 2010.

AMATO, F.; ARIOLA, M. Finite-time control of discrete-time linear systems. **IEEE Transactions on Automatic Control**, v. 50, n. 5, p. 724–729, 2005.

AMATO, F.; ARIOLA, M.; COSENTINO, C. Finite-time stability of linear time-varying systems: Analysis and controller design. **IEEE Transactions on Automatic Control**, v. 55, n. 4, p. 1003–1008, 2010.

AMATO, F.; ARIOLA, M.; DORATO, P. Finite-time control of linear systems subject to parametric uncertainties and disturbances. **Automatica**, v. 37, n. 9, p. 1459–1463, 2001.

ARMANINI, S. F.; KARÁSEK, M.; VISSER, C. C. de. Global LPV model identification of flapping-wing dynamics using flight data. *In*: **2018 AIAA Modeling and Simulation Technologies Conference**. Kissimmee, Florida: AIAA, 2018. p. 2156.

BAI, Y. *et al.* Finite-time high-order sliding mode control of supercavitating vehicle based on perturbation observer. **European Journal of Control**, Elsevier, v. 75, p. 100932, 2024.

BERTOLIN, A. L. *et al.* LMI-based stability tests for LPV and switched discrete-time linear systems through redundant equations. **IFAC-PapersOnLine**, Elsevier, v. 51, n. 26, p. 149–154, 2018.

CALAFIORE, G.; CAMPI, M. C. Uncertain convex programs: randomized solutions and confidence levels. **Mathematical Programming**, Springer, v. 102, p. 25–46, 2005.

CALAFIORE, G.; FAGIANO, L. Stochastic model predictive control of LPV systems via scenario optimization. **Automatica**, v. 49, n. 6, p. 1861–1866, 2013.

CAMPI, M.; GARATTI, S. The exact feasibility of randomized solutions of uncertain convex programs. **SIAM Journal on Optimization**, v. 19, n. 3, p. 1211–1230, 2008.

CAMPI, M.; GARATTI s. A sampling-and-discarding approach to chance-constrained optimization: Feasibility and optimality. **Journal of Optimization Theory and Applications**, v. 148, 2011.

CASAVOLA, A.; FAMULARO, D.; FRANZÈ, G. Predictive control of constrained nonlinear systems via LPV linear embeddings. **International Journal of Robust and Nonlinear Control: IFAC-Affiliated Journal**, Wiley Online Library, v. 13, n. 3-4, p. 281–294, 2003.

CHAE, Y.; RICLES, J. M.; SAUSE, R. Modeling of a large-scale magneto-rheological damper for seismic hazard mitigation. part ii: Semi-active mode. **Earthquake Engineering & Structural Dynamics**, v. 42, 2013.

CHAIB-DRAA, K. *et al.* Finite-time estimation algorithms for LPV discrete-time systems with application to output feedback stabilization. **Automatica**, v. 125, p. 109436, 2021.

CHEN, H.; NIE, Z.; YU, L. Parameter identification of modified bouc-wen model for MRF damper based on genetic algorithm and nonlinear least square method. *In*: **Proceedings of China SAE Congress 2021: Selected Papers**. Singapore: Springer Nature Singapore, 2022. v. 818, p. 686–697.

CURIE, E. **Madame Curie: A Biography by Eve Curie (Sheean V, trans)**. Garden City, NY: Doubleday, Duran & Company, Inc, 1937. Disponível em: https://archive.org/details/madamecurie0000unse/page/116/mode/2up.

DAAFOUZ, J.; BERNUSSOU, J. Parameter dependent Lyapunov functions for discrete time systems with time varying parametric uncertainties. **Systems & Control Letters**, v. 43, n. 5, p. 355–359, 2001.

DANIEL, C. *et al.* Magnetorheological damper for performance enhancement against seismic forces. *In*: SPRINGER. **Facing the Challenges in Structural Engineering: Proceedings of the 1st GeoMEast International Congress and Exhibition, Egypt 2017 on Sustainable Civil Infrastructures 1**. Egypt, 2018. p. 104–117.

DANIEL, G. **Identification of Systems**. Huntington, N.Y. : R. E. Krieger, 1976. ISBN 9780882753591. Disponível em: archive.org/details/identificationof0000grau/page/210/mode/1up?view=theater.

DANIELSON, C.; KLOEPPEL, J.; PETERSEN, C. Experimental validation of constrained spacecraft attitude planning via invariant sets. **Journal of Guidance, Control, and Dynamics**, v. 47, 2023.

DOMINGUEZ, A.; SEDAGHATI, R.; STIHARU, I. A new dynamic hysteresis model for magnetorheological dampers. **Smart materials and structures**, IOP Publishing, v. 15, n. 5, p. 1179, 2006.

DOMINGUEZ, A.; SEDAGHATI, R.; STIHARU, I. Modeling and application of MR dampers in semi-adaptive structures. **Computers & structures**, Elsevier, v. 86, n. 3-5, p. 407–415, 2008.

DUAN, G.-R.; YU, H.-H. **LMIs in control systems: analysis, design and applications**. Boca Raton, Florida, USA: CRC press, 2013. 483 p.

EFIMOV, D.; RAISSI, T.; ZOLGHADRI, A. Control of nonlinear and LPV systems: interval observer-based framework. **IEEE Transactions on Automatic Control**, IEEE, v. 58, n. 3, p. 773–778, 2013.

FREEMAN, J.; HASSAN, F.; MORTON., D. Kalman filter parameter identification: a practical approach. **Transactions of the Institute of Measurement and Control.**, v. 8, p. 24–28, 1986.

GEROMEL, J. C. **Differential Linear Matrix Inequalities**. Switzerland: Springer Nature, 2023.

GHAOUI, L. E.; NICULESCU, S.-I. **Advances in linear matrix inequality methods in control**. 3600 University City Science Center Philadelphia, PA, United States: SIAM, 1999. 316 p.

GUNASEKARAN, N. *et al.* Finite-time stability analysis and control of stochastic SIR epidemic model: A study of covid-19. **Biomedical Signal Processing and Control**, v. 86, p. 105123, 2023.

HA, Q.; ROYEL, S.; BALAGUER, C. Low-energy structures embedded with smart dampers. **Energy and Buildings**, Elsevier, v. 177, p. 375–384, 2018.

KHALID, M. *et al.* Nonlinear identification of a magneto-rheological damper based on dynamic neural networks. **Computer-Aided Civil and Infrastructure Engineering**, Wiley Online Library, v. 29, n. 3, p. 221–233, 2014.

KHALIL, H. K. **Control of nonlinear systems**. New York: Prentice Hall, NY, 2002.

LI, H.; FU, M. A linear matrix inequality approach to robust h/sub/spl infin//filtering. **IEEE Transactions on Signal Processing**, IEEE, v. 45, n. 9, p. 2338–2350, 1997.

LI, H.; WANG, J. Experimental investigation of the seismic control of a nonlinear soil-structure system using MR dampers. **Smart Materials and Structures**, IOP Publishing, v. 20, n. 8, p. 085026, 2011.

LI, X.; YANG, X.; SONG, S. Lyapunov conditions for finite-time stability of time-varying time-delay systems. **Automatica**, v. 103, p. 135–140, 2019.

LIU, Y.; YANG, J.; LI, C. Robust finite-time stability and stabilisation for switched linear parameter-varying systems and its application to bank-to-turn missiles. **IET Control Theory & Applications**, Wiley Online Library, v. 9, n. 14, p. 2171–2179, 2015.

LOFBERG, J. YALMIP: a toolbox for modeling and optimization in MATLAB. *In*: IEEE. **2004 IEEE International Conference on Robotics and Automation (IEEE Cat. No.04CH37508)**. Taipei, Taiwan, 2004. p. 284–289.

MA, Y.-j.; WU, B.-w.; WANG, Y.-E. Finite-time stability and finite-time boundedness of fractional order linear systems. **Neurocomputing**, Elsevier, v. 173, p. 2076–2082, 2016.

MASA'ID, A. *et al.* A review on vibration control strategies using magnetorheological materials actuators: Application perspective. *In*: MDPI. **Actuators**. Switzerland, 2023. v. 12, n. 3, p. 113.

MAYNE, D. Q. Optimal non-stationary estimation of the parameters of a linear system with Gaussian inputs. **Journal of Electronics and Control**, Taylor & Francis, v. 14, n. 1, p. 101–112, 1963.

MOSEK ApS. **The MOSEK optimization toolbox for MATLAB manual. Version 9.0.** Denmark, 2019. Disponível em: http://docs.mosek.com/9.0/toolbox/index.html.

NIE, L. *et al.* Finite-time bounded control for quadrotors with extended dissipative performance using a switched system approach. **Transactions of the Institute of Measurement and Control**, SAGE Publications Sage UK: London, England, v. 44, n. 13, p. 2511–2521, 2022.

OSTERTAG, E. **Mono- and Multivariable Control and Estimation.** Heidelberg, Berlin: Springer Berlin, 2011. ISSN 2192-4732.

PANDEY, A. P.; OLIVEIRA, M. C. de. On the necessity of LMI-based design conditions for discrete time LPV filters. **IEEE Transactions on Automatic Control**, IEEE, v. 63, n. 9, p. 3187–3188, 2018.

PENG, Y.; YANG, J.; LI, J. Parameter identification of modified bouc–wen model and analysis of size effect of magnetorheological dampers. **Journal of Intelligent Material Systems and Structures**, SAGE Publications Sage UK: London, England, v. 29, n. 7, p. 1464–1480, 2018.

ROSA, T. E.; MORAIS, C. F.; OLIVEIRA, R. C. New robust LMI synthesis conditions for mixed gain-scheduled reduced-order DOF control of discrete-time LPV systems. **International Journal of Robust and Nonlinear Control**, Wiley Online Library, v. 28, n. 18, p. 6122–6145, 2018.

ROTONDO, D.; NEJJARI, F.; PUIG, V. Robust state-feedback control of uncertain LPV systems: An LMI-based approach. **Journal of the Franklin Institute**, Elsevier, v. 351, n. 5, p. 2781–2803, 2014.

ŞAHIN, Ö. *et al.* A comparative evaluation of semi-active control algorithms for real-time seismic protection of buildings via magnetorheological fluid dampers. **Journal of Building Engineering**, Elsevier, v. 42, p. 102795, 2021.

SASTRY, S. **Nonlinear systems: analysis, stability, and control**. New York: Springer Science & Business Media, 2013. v. 10.

SCHILDBACH, G.; FAGIANO, L.; MORARI, M. Randomized solutions to convex programs with multiple chance constraints. **SIAM Journal on Optimization**, Society for Industrial & Applied Mathematics (SIAM), v. 23, n. 4, p. 2479–2501, jan. 2013.

SNYDER, R. A.; KAMATH, G. M.; WERELEY, N. M. Characterization and analysis of magnetorheological damper behavior under sinusoidal loading. **AIAA journal**, v. 39, n. 7, p. 1240–1253, 2001.

SOUZA, R. P. P. de *et al.* Inter-turn short-circuit fault diagnosis using robust adaptive parameter estimation. **International Journal of Electrical Power & Energy Systems**, Elsevier, v. 139, p. 107999, 2022.

TEMPO, R.; CALAFIORE, G.; DABBENE, F. **Randomized Algorithms for Analysis and Control of Uncertain Systems**. London: Springer London, 2004. 1-360 p.

TEMPO, R.; CALAFIORE, G.; DABBENE, F. **Randomized Algorithms for Analysis and Control of Uncertain Systems: With Applications**. New York, NY, USA: Springer, 2013.

TSOUROUKDISSIAN, A. R. *et al.* Modeling and identification of a small-scale magnetorheological damper. **Journal of Intelligent Material Systems and Structures**, Sage Publications Sage UK: London, England, v. 20, n. 7, p. 825–835, 2009.

VANANTWERP, J. G.; BRAATZ, R. D. A tutorial on linear and bilinear matrix inequalities. **Journal of process control**, Elsevier, v. 10, n. 4, p. 363–385, 2000.

VARGAS, A. *et al.* Shaking table attached to magnetorheological damper: Simulation and experiments for structural engineering. **Sensors (Basel)**, v. 22, n. 10, p. 3644, 2022.

VARGAS, A. N. *et al.* Robust stability of Markov jump linear systems through randomized evaluations. **Applied Mathematics and Computation**, v. 346, p. 287–294, 2019.

WEI, S.; WANG, J.; OU, J. Method for improving the neural network model of the magnetorheological damper. **Mechanical Systems and Signal Processing**, v. 149, p. 107316, 2021.

WEISS, L.; INFANTE, E. Finite time stability under perturbing forces and on product spaces. **IEEE Transactions on Automatic Control**, v. 12, n. 1, p. 54–59, 1967.

WU, F. A generalized lpv system analysis and control synthesis framework. **International Journal of Control**, Taylor & Francis, v. 74, n. 7, p. 745–759, 2001.

XU, Q.; ZHANG, N.; QI, W. Finite-time control for discrete-time nonlinear Markov switching LPV systems with dos attacks. **Applied Mathematics and Computation**, Elsevier, v. 443, p. 127783, 2023.

YU, M.; BIANCHI, F.; PIRODDI, L. A randomized method for the identification of switched narx systems. **Nonlinear Analysis: Hybrid Systems**, Elsevier, v. 49, p. 101364, 2023.

YUAN, X. *et al.* A review on structural development of magnetorheological fluid damper. **Shock and vibration**, Hindawi, v. 2019, 2019.

ZHANG, G. *et al.* A novel parametric model for nonlinear hysteretic behaviours with strain-stiffening of magnetorheological gel composite. **Composite Structures**, Elsevier, v. 318, p. 117082, 2023.

ZHANG, H.; WANG, R.; WANG, J. Polytopic LPV approaches for intelligent automotive systems: State of the art and future challenges. *In*: **Robust Gain-Scheduled Estimation and Control of Electrified Vehicles via LPV Technique**. Singapore: Springer, Singapore, 2023. p. 1–49.

ZHANG, X.; HAN, Q.; GE, X. Novel stability criteria for linear time-delay systems using Lyapunov-Krasovskii functionals with a cubic polynomial on time-varying delay. **IEEE/CAA Journal of Automatica Sinica**, v. 8, n. 6, p. 77, 2021.

ZHOU, B. Finite-time stability analysis and stabilization by bounded linear time-varying feedback. **Automatica**, v. 121, p. 109191, 2020.

ZHU, Y.; ZHENG, W. X. An integrated design approach for fault-tolerant control of switched lpv systems with actuator faults. **IEEE Transactions on Systems, Man, and Cybernetics: Systems**, v. 53, n. 2, p. 908–921, 2023.